PERGAMON

International Journal of Solids and Structures 39 (2002) 2477–2494

INTERNATIONAL JOURNAL OF SOLIDS and STRUCTURES

www.elsevier.com/locate/ijsolstr

On the dynamic behaviour of a piezoelectric laminate with multiple interfacial collinear cracks

Xiaohua Zhao, S.A. Meguid *

Engineering Mechanics and Design Laboratory, Department of Mechanical and Industrial Engineering, University of Toronto, 5 King's College Road, Toronto, Ont., Canada M5S 3G8

Received 14 June 2001; received in revised form 7 February 2002

Abstract

This paper investigates the dynamic behaviour of a piezoelectric laminate containing multiple interfacial collinear cracks subjected to steady-state electro-mechanical loads. Both the permeable and impermeable boundary conditions are examined and discussed. Based on the use of integral transform techniques, the problem is reduced to a set of singular integral equations, which can be solved using Chebyshev polynomial expansions. Numerical results are provided to show the effect of the geometry of interacting collinear cracks, the applied electric fields, the electric boundary conditions along the crack faces and the loading frequency on the resulting dynamic stress intensity and electric displacement intensity factors. © 2002 Published by Elsevier Science Ltd.

Keywords: Interface; Crack; Piezoelectric; Dynamic

1. Introduction

With the increasing usage of piezoelectric materials and composites as actuating and sensing devices in smart structures, where dynamic loading is dominant, much attention has been paid to their dynamic fracture behaviour. Shindo and Ozawa (1990) first investigated the steady state dynamic response of cracked piezoelectric materials under the action of incident plane harmonic waves. The dynamic Green's functions for anisotropic piezoelectric materials were derived by Norris (1994). Khutoryyansky and Sosa (1995) proposed dynamic representation formulas and fundamental solutions for piezoelectricity. Li and Mataga (1996a, 1996b) studied the problem of a semi-infinite crack propagating in an infinite piezoelectric medium. They investigated the effect of the propagating velocity of the crack on the crack tip fields. Narita and Shindo (1999) investigated the scattering of anti-plane shear waves by a finite crack in piezoelectric laminates. By the use of integral transforms and Copson–Sih's method, Chen and Karihaloo (1999) investigated the transient response of a finite crack in an infinite piezoelectric medium under the action of anti-plane mechanical loads and in-plane electric displacements. Meguid and Chen (2001), Wang and Yu

* Corresponding author. Fax: +1-416-978-7753.
E-mail address: meguid@mie.utoronto.ca (S.A. Meguid).

0020-7683/02/$ - see front matter © 2002 Published by Elsevier Science Ltd.
PII: S0020-7683(02)00154-3

(2000), and Shin et al. (2001) considered the dynamic crack problem in a piezoelectric strip under electro-mechanical impact. Meguid and Wang (1998) and Wang and Meguid (2000) studied the dynamic anti-plane interaction of cracks in a piezoelectric medium under incident shear wave loading.

Most piezoelectric devices in smart structures are surface-mounted, and debonding may take place along the interfaces between those devices and the host structures. It is, therefore, of great importance to investigate the effect of debonding on the coupled electro-mechanical behaviour of an integrated structure. Li et al. (2000) considered a moving crack at the interface between two dissimilar piezoelectric materials. Based on the use of the impermeable crack condition, Wang et al. (2000) analyzed a cracked piezoelectric laminate subjected to electro-mechanical impact loads. With a pseudo-incident wave method, Wang (2001) discussed the scattering of multiple interfacial cracks between two infinite piezoelectric mediums. In his study, the cracks were assumed to be permeable.

In this paper, we consider the dynamic behaviour of a piezoelectric laminate containing multiple interfacial collinear cracks subjected to steady-state electro-mechanical loads. Both the permeable and impermeable boundary conditions are considered and discussed. Based on the use of integral transform techniques, the problem is reduced to a set of singular integral equations, which can be solved using Chebyshev polynomial expansions. Numerical results are provided to show the effect of the geometry of interacting cracks, the applied electric fields, the electric boundary conditions along the crack faces and the loading frequency on the resulting dynamic stress intensity factor and electric displacement intensity factor.

2. Formulation of the problem

Consider the problem of a piezoelectric laminate containing n interfacial collinear cracks, as shown in Fig. 1. A set of Cartesian coordinates (x, y, z) is chosen such that the x-axis is directed along the crack line and y-axis is perpendicular to it. The poled piezoelectric strip, with the z-axis being the poling direction, occupies the region $(-h < y < 0, -\infty < x < +\infty)$. It is assumed that the laminate is subjected to a uniform shear stress $\tau_0 \exp(-i\omega t)$ at $y = -h$, h_1 and $-\infty < x < +\infty$. Furthermore, a uniform in-plane electric displacement $D_0 \exp(-i\omega t)$ is prescribed on the lower surface of the piezoelectric strip, resulting in a steady and coupled electric and stress wave field.

For the sake of convenience, the exponential harmonic factor $\exp(-i\omega t)$ will be suppressed and only the amplitude of different field variables will be considered. In this configuration, the piezoelectric boundary value problem is simplified considerably because only the out-of-plane displacement and the in-plane electric fields exist. The constitutive relation for the piezoelectric material can be expressed as

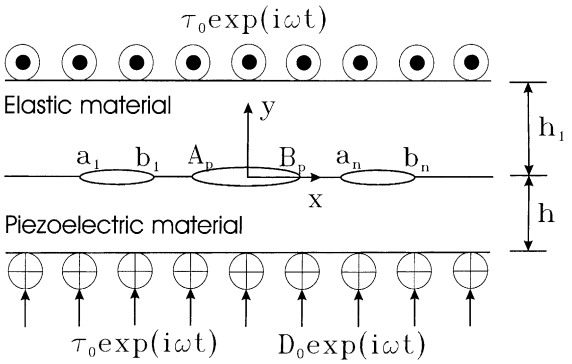

Fig. 1. Geometric configuration of the problem.

$$\tau_{xz} = c_{44}\frac{\partial w}{\partial x} + e_{15}\frac{\partial \phi}{\partial x}, \quad \tau_{yz} = c_{44}\frac{\partial w}{\partial y} + e_{15}\frac{\partial \phi}{\partial y} \tag{1}$$

and

$$D_x = e_{15}\frac{\partial w}{\partial x} - \kappa_{11}\frac{\partial \phi}{\partial x}, \quad D_y = e_{15}\frac{\partial w}{\partial y} - \kappa_{11}\frac{\partial \phi}{\partial y} \tag{2}$$

where τ_{xz} and τ_{yz} are the shear stress components, D_x and D_y are the electric displacements, w and ϕ are the mechanical displacement and electric potential, while c_{44}, e_{15} and κ_{11} are the elastic modulus, the piezoelectric constant and the dielectric constant of the piezoelectric material, respectively.

The equilibrium equation and the Maxwell equation for the piezoelectric material under anti-plane loading are given by

$$\frac{\partial \tau_{xz}}{\partial x} + \frac{\partial \tau_{yz}}{\partial y} + \rho\omega^2 w = 0 \tag{3}$$

$$\frac{\partial D_x}{\partial x} + \frac{\partial D_y}{\partial y} = 0 \tag{4}$$

where ρ is the density of the piezoelectric material.

Substituting Eqs. (1) and (2) into (3) and (4) results in the following governing equations:

$$\nabla^2 w + k_0^2 w = 0, \quad \kappa_{11}\nabla^2\phi = e_{15}\nabla^2 w \tag{5}$$

where $k_0 = \omega/c_2$, with $c_2 = \sqrt{\mu/\rho}$ and $\mu = c_{44} + e_{15}^2/\kappa_{11}$.

The constitutive relation for the elastic material can be written as

$$\tau_{xz1} = c_{441}\frac{\partial w_1}{\partial x}, \quad \tau_{yz1} = c_{441}\frac{\partial w_1}{\partial y} \tag{6}$$

where τ_{xz1} and τ_{yz1} are the shear stress components, w_1 and c_{441} are the displacement and the elastic modulus, respectively. The governing equation is given by

$$\nabla^2 w_1 + k_1^2 w_1 = 0 \tag{7}$$

in which $k_1 = \omega/c_{21}$, with $c_{21} = \sqrt{c_{441}/\rho_1}$ and ρ_1 is the density of the elastic material.

In the framework of linear theory, the present problem can be treated as the superposition of two sub-problems. Sub-problem (a) considers a crack-free piezoelectric laminate under the action of electro-mechanical loads on both surfaces. While sub-problem (b) concerns a piezoelectric laminate of multiple interfacial cracks, with the crack faces subjected to the electro-mechanical loads that cancel out the stress and the electric displacement induced by sub-problem (a).

Sub-problem (a) can be easily solved and therefore the detailed calculation is omitted. The stress and the electric displacement along the interface are found to be

$$\bar{\tau}_{yz}(x,0) = \frac{\tau_0[\mu k_0 \sin(k_0 h) + c_{441}k_1 \sin(k_1 h_1)] + e_{15}c_{441}k_1 D_0 \sin(k_1 h_1)[1-\cos(k_0 h)]/k_{11}}{\mu k_0 \cos(k_1 h_1)\sin(k_0 h) + c_{441}k_1 \sin(k_1 h_1)\cos(k_0 h)} \tag{8}$$

$$\overline{D}_y(x,0) = D_0 \tag{9}$$

Next, we discuss sub-problem (b) in detail. With the help of Fourier transforms, the solution of the governing equations (5) and (7) is given by

$$w(x,y) = \frac{1}{2\pi}\int_{-\infty}^{\infty}[A_1(\xi)\exp(-\gamma y) + A_2(\xi)\exp(\gamma y)]\exp(-\mathrm{i}\xi x)\,\mathrm{d}\xi \tag{10}$$

$$\phi(x,y) = \frac{e_{15}}{\kappa_{11}} w(x,y) + \psi(x,y) \tag{11}$$

$$\psi(x,y) = \frac{1}{2\pi} \int_{-\infty}^{\infty} [A_3(\xi) \exp(-|\xi|y) + A_4(\xi) \exp(|\xi|y)] \exp(-\mathrm{i}\xi x)\, \mathrm{d}\xi \tag{12}$$

$$w_1(x,y) = \frac{1}{2\pi} \int_{-\infty}^{\infty} [A_5(\xi) \exp(-\gamma_1 y) + A_6(\xi) \exp(\gamma_1 y)] \exp(-\mathrm{i}\xi x)\, \mathrm{d}\xi \tag{13}$$

where

$$\gamma = \begin{cases} \sqrt{\xi^2 - k_0^2} & |\xi| \geqslant k_0 \\ \mathrm{i}\sqrt{k_0^2 - \xi^2} & |\xi| < k_0 \end{cases}, \quad \gamma_1 = \begin{cases} \sqrt{\xi^2 - k_1^2} & |\xi| \geqslant k_1 \\ \mathrm{i}\sqrt{k_1^2 - \xi^2} & |\xi| < k_1 \end{cases} \tag{14}$$

From (1), (2) and (6), the stresses and electric displacements are obtained as follows:

$$\begin{aligned} \tau_{xz}(x,y) = & -\frac{\mu \mathrm{i}}{2\pi} \int_{-\infty}^{\infty} \xi [A_1(\xi) \exp(-\gamma y) + A_2(\xi) \exp(\gamma y)] \exp(-\mathrm{i}\xi x)\, \mathrm{d}\xi \\ & - \frac{e_{15}\mathrm{i}}{2\pi} \int_{-\infty}^{\infty} \xi [A_3(\xi) \exp(-|\xi|y) + A_4(\xi) \exp(|\xi|y)] \exp(-\mathrm{i}\xi x)\, \mathrm{d}\xi \end{aligned} \tag{15}$$

$$\begin{aligned} \tau_{yz}(x,y) = & \frac{\mu}{2\pi} \int_{-\infty}^{\infty} \gamma [-A_1(\xi) \exp(-\gamma y) + A_2(\xi) \exp(\gamma y)] \exp(-\mathrm{i}\xi x)\, \mathrm{d}\xi \\ & + \frac{e_{15}}{2\pi} \int_{-\infty}^{\infty} |\xi| [-A_3(\xi) \exp(-|\xi|y) + A_4(\xi) \exp(|\xi|y)] \exp(-\mathrm{i}\xi x)\, \mathrm{d}\xi \end{aligned} \tag{16}$$

$$D_x(x,y) = \frac{\kappa_{11}\mathrm{i}}{2\pi} \int_{-\infty}^{\infty} \xi [A_3(\xi) \exp(-|\xi|y) + A_4(\xi) \exp(|\xi|y)] \exp(-\mathrm{i}\xi x)\, \mathrm{d}\xi \tag{17}$$

$$D_y(x,y) = -\frac{\kappa_{11}}{2\pi} \int_{-\infty}^{\infty} |\xi| [-A_3(\xi) \exp(-|\xi|y) + A_4(\xi) \exp(|\xi|y)] \exp(-\mathrm{i}\xi x)\, \mathrm{d}\xi \tag{18}$$

$$\tau_{xz1}(x,y) = -\frac{c_{441}\mathrm{i}}{2\pi} \int_{-\infty}^{\infty} \xi [A_5(\xi) \exp(-\gamma_1 y) + A_6(\xi) \exp(\gamma_1 y)] \exp(-\mathrm{i}\xi x)\, \mathrm{d}\xi \tag{19}$$

$$\tau_{yz1}(x,y) = \frac{c_{441}}{2\pi} \int_{-\infty}^{\infty} \gamma_1 [-A_5(\xi) \exp(-\gamma_1 y) + A_6(\xi) \exp(\gamma_1 y)] \exp(-\mathrm{i}\xi x)\, \mathrm{d}\xi \tag{20}$$

In the above expressions, $A_j(\xi)$ $(j = 1\text{–}6)$ are unknown functions, which will be determined from boundary conditions.

In the theoretical studies of crack problems, the modelling of the electric boundary conditions along the crack faces is still an open problem. Generally, there are two well-accepted electric boundary conditions; namely: the permeable and impermeable boundary conditions. From the physical viewpoint, those two electric boundary conditions are the two extreme cases, with the permeable boundary condition representing the case where the crack faces are in complete contact and the impermeable boundary condition representing the case where the crack is open and filled with vacuum. For the present case, those two electric boundary conditions are examined and the corresponding discussions are presented in Sections 3 and 4, respectively.

3. Solution of the permeable crack problem

In this section, we consider the permeable crack problem. It is assumed that the surface of the elastic material is grounded, so that the boundary conditions for the permeable crack problem can be written as

$$\tau_{yz1}(x,h_1)=0,\quad -\infty<x<\infty \tag{21a}$$

$$\tau_{yz1}(x,0)=\tau_{yz}(x,0),\quad -\infty<x<\infty \tag{21b}$$

$$\phi(x,0)=0,\quad -\infty<x<\infty \tag{21c}$$

$$\tau_{yz1}(x,0)=-\bar{\tau}_{yz}(x,0),\qquad x\in(a_p,b_p),\quad p=1,2,\ldots,n \tag{21d}$$

$$w(x,0)=w_1(x,0),\quad x\notin(a_p,b_p) \tag{21e}$$

$$\tau_{yz}(x,-h)=0,\quad -\infty<x<\infty \tag{21f}$$

$$D_y(x,-h)=0,\quad -\infty<x<\infty \tag{21g}$$

Substituting (10)–(13), (16), (18) and (20) into (21a)–(21c) and (21f) and (21g), we find

$$A_2(\xi)=\exp(2\gamma h)A_1(\xi) \tag{22}$$

$$A_3(\xi)=-\frac{e_{15}[1+\exp(2\gamma h)]}{\kappa_{11}[1+\exp(2|\xi|h)]}A_1(\xi) \tag{23}$$

$$A_4(\xi)=-\frac{e_{15}[1+\exp(2\gamma h)]}{\kappa_{11}[1+\exp(2|\xi|h)]}\exp(2|\xi|h)A_1(\xi) \tag{24}$$

$$A_5(\xi)=\exp(2\gamma_1 h_1)A_6(\xi) \tag{25}$$

$$A_6(\xi)=\frac{\mu\gamma[\exp(2\gamma h)-1][1+\exp(2|\xi|h)]+e_{15}^2/\kappa_{11}|\xi|[1+\exp(2\gamma h)][1-\exp(2|\xi|h)]}{c_{441}\gamma_1[1+\exp(2|\xi|h)][1-\exp(2\gamma_1 h_1)]}A_1(\xi) \tag{26}$$

Denote that

$$\Delta w(x)=w_1(x,0)-w(x,0) \tag{27}$$

then, we have

$$\Delta w(x)=\begin{cases}0 & x\notin(a_k,b_k),\\ \Delta w_k(x) & x\in(a_k,b_k),\end{cases}\quad k=1,2,\ldots,n \tag{28}$$

To reduce the mixed boundary conditions (21d) and (21e) into an integral equation, we now introduce the following dislocation function

$$\varphi(x)=\frac{\mathrm{d}(\Delta w)}{\mathrm{d}x}=\begin{cases}0 & x\notin(a_k,b_k)\\ \varphi_k(x) & x\in(a_k,b_k)\end{cases} \tag{29}$$

where $\varphi_k(x)=\mathrm{d}(\Delta w_k)/\mathrm{d}x$. Then, from (21e) we have

$$\int_{a_p}^{b_p}\varphi_p(x)\,\mathrm{d}x=0,\quad p=1,2,\ldots,n \tag{30}$$

Substitution of (10) and (13) into (29) yields

$$\varphi(x) = -\frac{1}{2\pi}\int_{-\infty}^{\infty} \mathrm{i}\xi[A_5(\xi) + A_6(\xi) - A_1(\xi) - A_2(\xi)]\exp(-\mathrm{i}\xi x)\,\mathrm{d}\xi \tag{31}$$

From the above equation and the definition of Fourier transform, we obtain

$$A_5(\xi) + A_6(\xi) - A_1(\xi) - A_2(\xi) = -\frac{1}{\mathrm{i}\xi}\sum_{k=1}^{n}\int_{a_k}^{b_k}\varphi_k(\alpha)\exp(\mathrm{i}\xi\alpha)\,\mathrm{d}\alpha \tag{32}$$

Further, from (22)–(26) and (32), we have

$$A_1(\xi) = -\frac{c_{441}\gamma_1[1+\exp(2|\xi|h)][1-\exp(2\gamma_1 h_1)]}{\mathrm{i}\xi F_1(\xi)}\sum_{k=1}^{n}\int_{a_k}^{b_k}\varphi_k(\alpha)\exp(\mathrm{i}\xi\alpha)\,\mathrm{d}\alpha \tag{33}$$

where

$$\begin{aligned} F_1(\xi) = {} & \frac{e_{15}^2}{\kappa_{11}}|\xi|[1+\exp(2\gamma h)][1-\exp(2|\xi|h)][1+\exp(2\gamma_1 h_1)] + [1+\exp(2|\xi|h)] \\ & \times\{\mu\gamma[1+\exp(2\gamma_1 h_1)][\exp(2\gamma h)-1] - c_{441}\gamma_1[1-\exp(2\gamma_1 h_1)][1+\exp(2\gamma h)]\} \end{aligned} \tag{34}$$

By using Eq. (21d), it is shown that

$$\begin{aligned} & \int_{-\infty}^{\infty}\frac{\gamma_1 F_2(\xi)\exp(-\mathrm{i}\xi x)}{\mathrm{i}\xi F_1(\xi)}\sum_{k=1}^{n}\int_{a_k}^{b_k}\varphi_k(\alpha)\exp(\mathrm{i}\xi\alpha)\,\mathrm{d}\alpha\,\mathrm{d}\xi = \frac{2\pi}{c_{441}}\bar{\tau}_{yz}(x,0), \\ & \quad x\in(a_p,b_p), \quad p=1,2,\ldots,n \end{aligned} \tag{35}$$

where

$$F_2(\xi) = [1-\exp(2\gamma_1 h_1)]\left\{\mu\gamma[1+\exp(2|\xi|h)][\exp(2\gamma h)-1] + e_{15}^2/\kappa_{11}|\xi|[1-\exp(2|\xi|h)][1+\exp(2\gamma h)]\right\} \tag{36}$$

After performing the appropriate asymptotic analysis, the following result can be obtained:

$$\lim_{|\xi|\to\infty}\frac{\gamma_1 F_2(\xi)}{\xi F_1(\xi)} = -\frac{c_{44}}{c_{44}+c_{441}}\mathrm{sign}(\xi) \tag{37}$$

By making use of Eq. (37) and defining that

$$\alpha = \frac{b_k - a_k}{2}\eta + \frac{b_k + a_k}{2} = e_k\eta + d_k \tag{38}$$

$$x = \frac{b_p - a_p}{2}u + \frac{b_p + a_p}{2} = e_p u + d_p \tag{39}$$

Eq. (35) becomes

$$\int_{-1}^{1}\frac{\varphi_p(\eta)}{\eta-u}\,\mathrm{d}\eta + \sum_{k=1}^{n}\int_{-1}^{1}Q_{pk}(\eta,u)\varphi_k(\eta)\,\mathrm{d}\eta = -\frac{\pi(c_{44}+c_{441})}{c_{44}c_{441}}\bar{\tau}_{yz}(u,0), \quad |u|<1,\ \ p=1,2,\ldots,n \tag{40}$$

where

$$\begin{aligned} Q_{pk}(\eta,u) = {} & \frac{e_k}{e_k\eta - e_p u + (d_k - d_p)} - \frac{\delta_{pk}}{\eta-u} - \int_0^{\infty} e_k\left[\frac{(c_{44}+c_{441})\gamma_1 F_2(\xi)}{c_{44}\xi F_1(\xi)} + 1\right] \\ & \times\sin\left[\xi(e_k\eta + d_k) - \xi(e_p u + d_p)\right]\mathrm{d}\xi \end{aligned} \tag{41}$$

Eq. (30) can be written as

$$\int_{-1}^{1} \varphi_p(\eta)\,\mathrm{d}\eta = 0, \quad p = 1,2,\ldots,n \tag{42}$$

Eq. (40) is a singular integral equation of the first kind, its solution includes the well-known square-root singularity and can be expressed as

$$\varphi_k(\eta) = \sum_{j=0}^{\infty} \frac{B_{kj}}{\sqrt{1-\eta^2}} T_j(\eta) \tag{43}$$

where $T_j(\eta)$ are Chebyshev polynomials of the first kind and B_{kj} are unknown constants. From the orthogonality conditions of Chebyshev polynomials, Eq. (42) leads to $B_{k0} = 0$. Substituting Eq. (43) into (40), the following algebraic equation for B_{kj} is obtained:

$$\sum_{j=1}^{\infty} B_{pj} U_{j-1}(u) + \sum_{k=1}^{n} \sum_{j=1}^{\infty} B_{kj} L_{pkj}(u) = -\frac{c_{44}+c_{441}}{c_{44}c_{441}} \bar{\tau}_{yz}(u,0), \quad |u| < 1 \;\; p = 1,2,\ldots,n \tag{44}$$

where $U_j(u)$ represent Chebyshev polynomials of the second kind, and

$$L_{pkj}(u) = \int_{-1}^{1} \frac{T_j(\eta)}{\pi\sqrt{1-\eta^2}} Q_{pk}(\eta,u)\,\mathrm{d}\eta \tag{45}$$

Truncating the Chebyshev polynomials in Eq. (44) to the Nth term and assuming that Eq. (44) is satisfied at N collocation points along the crack faces,

$$u_m = \cos\left(\frac{m\pi}{N+1}\right), \quad m = 1,2,\ldots,N \tag{46}$$

Eq. (44) can be reduced to a linear algebraic system of equations of the following form:

$$\sum_{j=1}^{N} B_{pj} \sin\left(\frac{mj\pi}{N+1}\right) \Big/ \sin\left(\frac{m\pi}{N+1}\right) + \sum_{k=1}^{n} \sum_{j=1}^{N} B_{kj} L_{pkj}(u_m) = -\frac{c_{44}+c_{441}}{c_{44}c_{441}} \bar{\tau}_{yz}(u_m,0),$$
$$m = 1,2,\ldots,N \;\text{ and }\; p = 1,2,\ldots,n \tag{47}$$

Once B_{kj} are determined from (47), the stress components can be obtained. Then, the dynamic stress intensity factors of crack p can be evaluated using the following expressions:

$$K_{\mathrm{III}}^{R} = \lim_{x\to b_p^+} \sqrt{2\pi(x-b_p)}\,\tau_{yz}(x,0) = -\frac{c_{44}c_{441}}{c_{44}+c_{441}} \sqrt{\frac{\pi(b_p-a_p)}{2}} \sum_{j=1}^{\infty} B_{pj} \tag{48}$$

$$K_{\mathrm{III}}^{L} = \lim_{x\to a_p^-} \sqrt{2\pi(a_p-x)}\,\tau_{yz}(x,0) = \frac{c_{44}c_{441}}{c_{44}+c_{441}} \sqrt{\frac{\pi(b_p-a_p)}{2}} \sum_{j=1}^{\infty} (-1)^j B_{pj} \tag{49}$$

4. Solution of the impermeable crack problem

Consider now the impermeable crack problem. The boundary conditions for the problem can be expressed as

$$\tau_{yz1}(x,h_1) = 0, \quad -\infty < x < \infty \tag{50a}$$

$$\tau_{yz1}(x,0) = \tau_{yz}(x,0), \quad -\infty < x < \infty \tag{50b}$$

$$\tau_{yz}(x,0) = -\bar{\tau}_{yz}(x,0), \quad x \in (a_p, b_p) \tag{50c}$$

$$w(x,0) = w_1(x,0), \quad x \notin (a_p, b_p) \tag{50d}$$

$$D_y(x,0) = -D_0, \quad x \in (a_p, b_p) \tag{50e}$$

$$\phi(x,0) = 0, \quad x \notin (a_p, b_p) \tag{50f}$$

$$\tau_{yz}(x,-h) = 0, \quad -\infty < x < \infty \tag{50g}$$

$$D_y(x,-h) = 0, \quad -\infty < x < \infty \tag{50h}$$

From (50a), (50b), (50g) and (50h), it can be seen that

$$A_2(\xi) = A_1(\xi)\exp(2\gamma h) \tag{51}$$

$$A_4(\xi) = A_3(\xi)\exp(2|\xi|h) \tag{52}$$

$$A_5(\xi) = \frac{\mu\gamma[\exp(2\gamma h) - 1]\exp(2\gamma_1 h_1)}{c_{441}\gamma_1[1 - \exp(2\gamma_1 h_1)]}A_1(\xi) + \frac{e_{15}|\xi|[\exp(2|\xi|h) - 1]\exp(2\gamma_1 h_1)}{c_{441}\gamma_1[1 - \exp(2\gamma_1 h_1)]}A_3(\xi) \tag{53}$$

$$A_6(\xi) = \frac{\mu\gamma[\exp(2\gamma h) - 1]}{c_{441}\gamma_1[1 - \exp(2\gamma_1 h_1)]}A_1(\xi) + \frac{e_{15}|\xi|[\exp(2|\xi|h) - 1]}{c_{441}\gamma_1[1 - \exp(2\gamma_1 h_1)]}A_3(\xi) \tag{54}$$

Let us again introduce the following dislocation function:

$$\varphi_1(x) = \frac{\mathrm{d}}{\mathrm{d}x}[w_1(x,0) - w(x,0)] \tag{55}$$

and the following definition:

$$\varphi_2(x) = -\frac{\mathrm{d}\phi(x,0)}{\mathrm{d}x} \tag{56}$$

According to Eqs. (50d) and (50f), those two functions can be written as

$$\varphi_1(x) = \begin{cases} 0 & x \notin (a_k, b_k) \\ \varphi_{1k}(x) & x \in (a_k, b_k) \end{cases} \tag{57}$$

$$\varphi_2(x) = \begin{cases} 0 & x \notin (a_k, b_k) \\ \varphi_{2k}(x) & x \in (a_k, b_k) \end{cases} \tag{58}$$

where $\varphi_{1k}(x) = \mathrm{d}(\Delta w_k)/\mathrm{d}x$, $\varphi_{2k}(x) = -\mathrm{d}\phi_k(x)/\mathrm{d}x$, and they must satisfy

$$\int_{a_p}^{b_p} \varphi_{1p}(x)\mathrm{d}x = 0, \quad p = 1, 2, \ldots, n \tag{59}$$

$$\int_{a_p}^{b_p} \varphi_{2p}(x)\mathrm{d}x = 0, \quad p = 1, 2, \ldots, n \tag{60}$$

By using Eqs. (55), (56), (10)–(13), and the definition of Fourier transform, we obtain

$$[1+\exp(2\gamma_1 h_1)]A_6(\xi)-[1+\exp(2\gamma h)]A_1(\xi)=-\frac{1}{\mathrm{i}\xi}\sum_{k=1}^{n}\int_{a_k}^{b_k}\varphi_{1k}(\alpha)\exp(\mathrm{i}\xi\alpha)\,\mathrm{d}\alpha \tag{61}$$

$$\frac{e_{15}}{\kappa_{11}}[1+\exp(2\gamma h)]A_1(\xi)+[1+\exp(2|\xi|h)]A_3(\xi)=\frac{1}{\mathrm{i}\xi}\sum_{k=1}^{n}\int_{a_k}^{b_k}\varphi_{2k}(\alpha)\exp(\mathrm{i}\xi\alpha)\,\mathrm{d}\alpha \tag{62}$$

Substitution of (51)–(54) into (61) and (62) yields

$$\begin{aligned}A_1(\xi)=&-\frac{c_{441}\gamma_1[1+\exp(2|\xi|h)][1-\exp(2\gamma_1 h_1)]}{\mathrm{i}\xi F_1(\xi)}\sum_{k=1}^{n}\int_{a_k}^{b_k}\varphi_{1k}(\alpha)\exp(\mathrm{i}\xi\alpha)\,\mathrm{d}\alpha\\&-\frac{e_{15}|\xi|[\exp(2|\xi|h)-1][1+\exp(2\gamma_1 h_1)]}{\mathrm{i}\xi F_1(\xi)}\sum_{k=1}^{n}\int_{a_k}^{b_k}\varphi_{2k}(\alpha)\exp(\mathrm{i}\xi\alpha)\,\mathrm{d}\alpha\end{aligned} \tag{63}$$

$$\begin{aligned}A_3(\xi)=&\frac{c_{441}e_{15}\gamma_1[1+\exp(2\gamma h)][1-\exp(2\gamma_1 h_1)]}{\mathrm{i}\kappa_{11}\xi F_1(\xi)}\sum_{k=1}^{n}\int_{a_k}^{b_k}\varphi_{1k}(\alpha)\exp(\mathrm{i}\xi\alpha)\,\mathrm{d}\alpha\\&+\frac{1}{\mathrm{i}\xi F_1(\xi)}\{\mu\gamma[\exp(2\gamma h)-1][1+\exp(2\gamma_1 h_1)]-c_{441}\gamma_1[1+\exp(2\gamma h)][1-\exp(2\gamma_1 h_1)]\}\\&\times\sum_{k=1}^{n}\int_{a_k}^{b_k}\varphi_{2k}(\alpha)\exp(\mathrm{i}\xi\alpha)\,\mathrm{d}\alpha\end{aligned} \tag{64}$$

From (50c) and (50e), we have

$$\int_{-\infty}^{\infty}\gamma[\exp(2\gamma h)-1]A_1(\xi)\exp(-\mathrm{i}\xi x)\,\mathrm{d}\xi=-\frac{2\pi}{\mu}\left[\bar{\tau}_{yz}(x,0)+\frac{e_{15}}{k_{11}}D_0\right],\quad x\in(a_p,b_p) \tag{65}$$

$$\int_{-\infty}^{\infty}|\xi|[\exp(2|\xi|h)-1]A_3(\xi)\exp(-\mathrm{i}\xi x)\,\mathrm{d}\xi=\frac{2\pi}{k_{11}}D_0,\quad x\in(a_p,b_p) \tag{66}$$

By substituting Eqs. (63) and (64) into (65) and (66), we obtain

$$\begin{aligned}&\frac{1}{\mathrm{i}}\int_{-\infty}^{\infty}a_{11}(\xi)\exp(-\mathrm{i}\xi x)\sum_{k=1}^{n}\int_{a_k}^{b_k}\varphi_{1k}(\alpha)\exp(\mathrm{i}\xi\alpha)\,\mathrm{d}\alpha\,\mathrm{d}\xi+\frac{1}{\mathrm{i}}\int_{-\infty}^{\infty}a_{12}(\xi)\exp(-\mathrm{i}\xi x)\\&\quad\times\sum_{k=1}^{n}\int_{a_k}^{b_k}\varphi_{2k}(\alpha)\exp(\mathrm{i}\xi\alpha)\,\mathrm{d}\alpha\,\mathrm{d}\xi=\frac{2\pi}{\mu}\left[\bar{\tau}_{yz}(x,0)+\frac{e_{15}}{k_{11}}D_0\right],\quad x\in(a_p,b_p)\end{aligned} \tag{67}$$

$$\begin{aligned}&\frac{1}{\mathrm{i}}\int_{-\infty}^{\infty}a_{21}(\xi)\exp(-\mathrm{i}\xi x)\sum_{k=1}^{n}\int_{a_k}^{b_k}\varphi_{1k}(\alpha)\exp(\mathrm{i}\xi\alpha)]\,\mathrm{d}\alpha\,\mathrm{d}\xi+\frac{1}{\mathrm{i}}\int_{-\infty}^{\infty}a_{22}(\xi)\exp(-\mathrm{i}\xi x)\\&\quad\times\sum_{k=1}^{n}\int_{a_k}^{b_k}\varphi_{2k}(\alpha)\exp(\mathrm{i}\xi\alpha)\,\mathrm{d}\alpha\,\mathrm{d}\xi=\frac{2\pi}{k_{11}}D_0,\quad x\in(a_p,b_p)\end{aligned} \tag{68}$$

where

$$a_{11}(\xi)=\frac{c_{441}\gamma\gamma_1[1+\exp(2|\xi|h)][\exp(2\gamma h)-1][1-\exp(2\gamma_1 h_1)]}{\xi F_1(\xi)} \tag{69}$$

$$a_{12}(\xi)=\frac{e_{15}|\xi|\gamma[\exp(2|\xi|h)-1][\exp(2\gamma h)-1][1+\exp(2\gamma_1 h_1)]}{\xi F_1(\xi)} \tag{70}$$

$$a_{21}(\xi)=\frac{e_{15}c_{441}|\xi|\gamma_1[\exp(2|\xi|h)-1][\exp(2\gamma h)+1][1-\exp(2\gamma_1 h_1)]}{\kappa_{11}\xi F_1(\xi)} \tag{71}$$

$$a_{22}(\xi)=\frac{|\xi|[\exp(2|\xi|h)-1]}{\xi F_1(\xi)}\{\mu\gamma[\exp(2\gamma h)-1][1+\exp(2\gamma_1 h_1)]-c_{441}\gamma_1[1+\exp(2\gamma h)][1-\exp(2\gamma_1 h_1)]\} \tag{72}$$

Performing appropriate asymptotic analysis leads to

$$\lim_{|\xi|\to\infty} a_{11}(\xi)=-\frac{c_{441}}{c_{44}+c_{441}}\operatorname{sign}(\xi) \tag{73}$$

$$\lim_{|\xi|\to\infty} a_{12}(\xi)=\frac{e_{15}}{c_{44}+c_{441}}\operatorname{sign}(\xi) \tag{74}$$

$$\lim_{|\xi|\to\infty} a_{21}(\xi)=-\frac{e_{15}c_{441}}{\kappa_{11}(c_{44}+c_{441})}\operatorname{sign}(\xi) \tag{75}$$

$$\lim_{|\xi|\to\infty} a_{22}(\xi)=\left[1+\frac{e_{15}^2}{\kappa_{11}(c_{44}+c_{441})}\right]\operatorname{sign}(\xi) \tag{76}$$

By the use of (38) and (39), and from (67) and (68) and (73)–(76), we have the following singular integral equations:

$$\begin{aligned}&\int_{-1}^{1}\frac{\varphi_{1p}(\eta)}{\eta-u}\,\mathrm{d}\eta-\frac{e_{15}}{c_{441}}\int_{-1}^{1}\frac{\varphi_{2p}(\eta)}{\eta-u}\,\mathrm{d}\eta+\sum_{k=1}^{n}\int_{-1}^{1}Q_{11pk}(\eta,u)\varphi_{1k}(\eta)\,\mathrm{d}\eta-\sum_{k=1}^{n}\int_{-1}^{1}Q_{12pk}(\eta,u)\varphi_{2k}(\eta)\,\mathrm{d}\eta\\&\quad=-\frac{\pi(c_{44}+c_{441})}{\mu c_{441}}\left[\bar{\tau}_{yz}(u,0)+\frac{e_{15}}{k_{11}}D_0\right],\quad |u|<1\end{aligned} \tag{77}$$

$$\begin{aligned}&-\int_{-1}^{1}\frac{\varphi_{1p}(\eta)}{\eta-u}\,\mathrm{d}\eta+\frac{k_{11}(\mu+c_{441})}{e_{15}c_{441}}\int_{-1}^{1}\frac{\varphi_{2p}(\eta)}{\eta-u}\,\mathrm{d}\eta+\sum_{k=1}^{n}\int_{-1}^{1}Q_{21pk}(\eta,u)\varphi_{1k}(\eta)\,\mathrm{d}\eta\\&\quad+\sum_{k=1}^{n}\int_{-1}^{1}Q_{22pk}(\eta,u)\varphi_{2k}(\eta)\,\mathrm{d}\eta=\frac{\pi(c_{44}+c_{441})}{e_{15}c_{441}}D_0,\quad |u|<1\end{aligned} \tag{78}$$

where

$$\begin{aligned}Q_{11pk}(\eta,u)=&\frac{e_k}{e_k\eta-e_pu+(d_k-d_p)}-\frac{\delta_{pk}}{\eta-u}-\int_0^{\infty}e_k\left[\frac{c_{44}+c_{441}}{c_{441}}a_{11}(\xi)+1\right]\\&\times\sin\left[\xi(e_k\eta+d_k)-\xi(e_pu+d_p)\right]\mathrm{d}\xi\end{aligned} \tag{79}$$

$$\begin{aligned}Q_{12pk}(\eta,u)=&\frac{e_{15}}{c_{441}}\left[\frac{e_k}{e_k\eta-e_pu+(d_k-d_p)}-\frac{\delta_{pk}}{\eta-u}\right]+\int_0^{\infty}e_k\left[\frac{c_{44}+c_{441}}{c_{441}}a_{12}(\xi)-\frac{e_{15}}{c_{441}}\right]\\&\times\sin\left[\xi(e_k\eta+d_k)-\xi(e_pu+d_p)\right]\mathrm{d}\xi\end{aligned} \tag{80}$$

$$Q_{21pk}(\eta,u) = -\frac{e_k}{e_k\eta - e_p u + (d_k - d_p)} + \frac{\delta_{pk}}{\eta - u} + \int_0^\infty e_k\left[\frac{k_{11}(c_{44}+c_{441})}{e_{15}c_{441}}a_{21}(\xi) + 1\right] \times \sin\left[\xi(e_k\eta + d_k) - \xi(e_p u + d_p)\right]\mathrm{d}\xi \tag{81}$$

$$Q_{22pk}(\eta,u) = \frac{k_{11}(\mu + c_{441})}{e_{15}c_{441}}\left[\frac{e_k}{e_k\eta - e_p u + (d_k - d_p)} - \frac{\delta_{pk}}{\eta - u}\right] + \int_0^\infty e_k\left[\frac{k_{11}(c_{44}+c_{441})}{e_{15}c_{441}}a_{22}(\xi) - \frac{k_{11}(\mu + c_{441})}{e_{15}c_{441}}\right]\sin\left[\xi(e_k\eta + d_k) - \xi(e_p u + d_p)\right]\mathrm{d}\xi \tag{82}$$

We also have

$$\int_{-1}^{1}\varphi_{lp}(\eta)\,\mathrm{d}\eta = 0, \qquad \int_{-1}^{1}\varphi_{2p}(\eta)\,\mathrm{d}\eta = 0, \quad p = 1,2,\ldots,n \tag{83}$$

In a similar fashion to Section 3, the functions $\varphi_{1k}(\eta)$ and $\varphi_{2k}(\eta)$ are defined in terms of the Chebyshev polynomials:

$$\varphi_{1k}(\eta) = \sum_{j=0}^{\infty}\frac{B_{kj}}{\sqrt{1-\eta^2}}T_j(\eta), \quad \varphi_{2k}(\eta) = \sum_{j=0}^{\infty}\frac{E_{kj}}{\sqrt{1-\eta^2}}T_j(\eta) \tag{84}$$

From (83), it follows that $B_{k0} = E_{k0} = 0$. By truncating the series to a reasonable number of terms and by using a simple collocation technique, we can determine the remaining unknowns using the following algebraic equations:

$$\sum_{j=1}^{N}\left[\frac{\sin\left(\frac{mj\pi}{N+1}\right)}{\sin\left(\frac{m\pi}{N+1}\right)}\right]B_{pj} - \frac{e_{15}}{c_{441}}\sum_{j=1}^{N}\left[\frac{\sin\left(\frac{mj\pi}{N+1}\right)}{\sin\left(\frac{m\pi}{N+1}\right)}\right]E_{pj} + \sum_{k=1}^{n}\sum_{j=1}^{N}L_{11pkj}(u_m)B_{kj} - \sum_{k=1}^{n}\sum_{j=1}^{N}L_{12pkj}(u_m)E_{kj} = -\frac{c_{44}+c_{441}}{\mu c_{441}}\left[\bar{\tau}_{yz}(u_m,0) + \frac{e_{15}}{k_{11}}D_0\right] \tag{85}$$

$$-\sum_{j=1}^{N}\left[\frac{\sin\left(\frac{mj\pi}{N+1}\right)}{\sin\left(\frac{m\pi}{N+1}\right)}\right]B_{pj} + \frac{k_{11}(\mu+c_{441})}{e_{15}c_{441}}\sum_{j=1}^{N}\left[\frac{\sin\left(\frac{mj\pi}{N+1}\right)}{\sin\left(\frac{m\pi}{N+1}\right)}\right]E_{pj} + \sum_{k=1}^{n}\sum_{j=1}^{N}L_{21pkj}(u_m)B_{kj} + \sum_{k=1}^{n}\sum_{j=1}^{N}L_{22pkj}(u_m)E_{kj} = \frac{c_{44}+c_{441}}{e_{15}c_{441}}D_0, \quad p = 1,2,\ldots,n \text{ and } m = 1,2,\ldots,N \tag{86}$$

where

$$L_{rspkj}(u_m) = \int_{-1}^{1}\frac{1}{\pi\sqrt{1-\eta^2}}Q_{rspk}(\eta,u_m)T_j(\eta)\,\mathrm{d}\eta, \quad r,s = 1,2 \tag{87}$$

Based on the solutions of (85) and (86), the dynamic stress intensity factors and electric displacement intensity factors of crack p can be obtained, as follows:

$$K_{\mathrm{III}}^R = \lim_{x\to b_p^+}\sqrt{2\pi(x-b_p)}\tau_{yz}(x,0) = \frac{\mu}{c_{44}+c_{441}}\sqrt{\frac{\pi(b_p-a_p)}{2}}\left(-c_{441}\sum_{j=1}^{\infty}B_{pj} + e_{15}\sum_{j=1}^{\infty}E_{pj}\right) - \frac{e_{15}}{\kappa_{11}}K_D^R \tag{88}$$

$$K_D^R = \lim_{x\to b_p^+}\sqrt{2\pi(x-b_p)}D_y(x,0)$$
$$= \frac{1}{c_{44}+c_{441}}\sqrt{\frac{\pi(b_p-a_p)}{2}}\left[-e_{15}c_{441}\sum_{j=1}^{\infty}B_{pj}+k_{11}(\mu+c_{441})\sum_{j=1}^{\infty}E_{pj}\right] \tag{89}$$

$$K_{\mathrm{III}}^L = \lim_{x\to a_p^-}\sqrt{2\pi(a_p-x)}\tau_{yz}(x,0)$$
$$= \frac{\mu}{c_{44}+c_{441}}\sqrt{\frac{\pi(b_p-a_p)}{2}}\left[c_{441}\sum_{j=1}^{\infty}(-1)^j B_{pj}-e_{15}\sum_{j=1}^{\infty}(-1)^j E_{pj}\right]-\frac{e_{15}}{\kappa_{11}}K_D^L \tag{90}$$

$$K_D^L = \lim_{x\to a_p^-}\sqrt{2\pi(a_p-x)}D_y(x,0)$$
$$= \frac{1}{c_{44}+c_{441}}\sqrt{\frac{\pi(b_p-a_p)}{2}}\left[e_{15}c_{441}\sum_{j=1}^{\infty}(-1)^j B_{pj}-k_{11}(\mu+c_{441})\sum_{j=1}^{\infty}(-1)^j E_{pj}\right] \tag{91}$$

5. Numerical results and discussions

Numerical calculations have been carried out to show the influence of the pertinent parameters. In the following examples, the piezoelectric material is assumed to be PZT-4, and the elastic material is assumed to be aluminium. The elastic, piezoelectric and dielectric properties of the materials are as follows (Narita and Shindo, 1999):

$$c_{44} = 2.56\times10^{10}\ \mathrm{N/m^2},\quad e_{15} = 12.7\ \mathrm{C/m^2},\quad \kappa_{11} = 64.6\times10^{-10}\ \mathrm{C/vm},\quad \rho = 7500\ \mathrm{kg/m^3};$$
$$c_{441} = 2.65\times10^{10}\ \mathrm{N/m^2},\quad \rho_1 = 2706\ \mathrm{kg/m^3}.$$

To check the convergence of the expansions in (43) and (84), a number of runs with varying number of terms were used. We found that good convergence (2% difference between two successive runs) can be reached when the number exceeds 15 terms. In all our calculations, we used twenty terms.

5.1. The single crack solution

Let us now restrict our attention to the single crack solution. It is assumed that $a_1 = -a$ and $b_1 = a$. Numerical results are shown in Figs. 2–11. In these figures, normalized parameters are used with SIF $= K_{\mathrm{III}}/(\tau_0\sqrt{\pi a})$, EDIF $= K_D/(D_0\sqrt{\pi a})$, and Dh $= e_{15}D_0/(\kappa_{11}\tau_0)$.

Figs. 2–4 show the results of the permeable crack problem. Specifically, Fig. 2 displays the variation of the SIF with k_0h for various h_1/h at $a/h = 0.6$ and Dh $= 0$. In the case of $h_1 = h$, it is seen that for lower frequencies, the dynamic SIF increases gradually with increasing k_0h. When the frequency k_0h approaches 1.2, an intense vibration takes place, which is reflected in the fact that the SIF changes sharply. This phenomenon can also be observed for $h_1 = 5h$ and $h_1 = 10h$.

Fig. 3 shows the influence of the applied electric fields on the dynamic stress intensity factor. It is seen that when the frequency of the applied electro-mechanical loads is low ($k_0h < 1.2$), the effect of electric fields is negligible. However, when the frequency increases, the effect becomes obvious. It is also seen that both the positive electric field (Dh $= 1.0$) and the negative electric field (Dh $= -1.0$) can induce the increase or decrease of the dynamic stress intensity factor, depending on the value of k_0h.

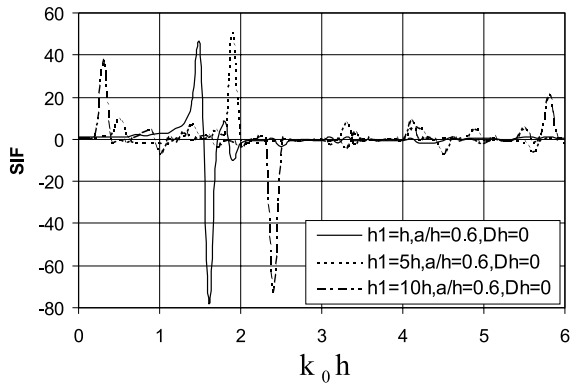

Fig. 2. Normalized SIF versus k_0h for various h_1/h assuming the permeable boundary condition.

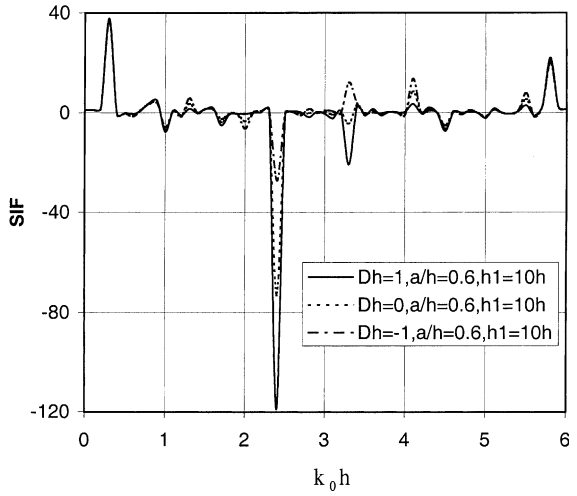

Fig. 3. Normalized SIF versus k_0h for various Dh assuming the permeable boundary condition.

The effects of crack geometry on the dynamic stress intensity factor are shown in Fig. 4. As can be seen from the figure, the SIFs for the three cracks have almost the same value for lower frequencies. With the increase in frequency, a significant difference is observed. In some specific ranges of frequencies, the SIF for $a/h = 0.2$ is much bigger than that for $a/h = 0.6$ and 1.0. For example, when $k_0h = 1.7$, the SIFs for $a/h = 0.2$, 0.6 and 1.0 are 32.67, 5.13 and 1.63, respectively. The related $K_{III}/(\tau_0\sqrt{\pi})$ are 14.60, 3.98 and 1.63, respectively. The inference of this is that small cracks are more likely to propagate and cause damage to the structure than larger cracks in those ranges of frequencies.

The results of the impermeable crack problem are presented in Figs. 5,6 and 8. Generally, similar observations can be deduced from Figs. 5–7. However, the frequency of an intense vibration increases, as is depicted in Figs. 5 and 6. In addition, the effect of the applied electric field on the dynamic SIF is more pronounced. The effect of crack geometry on the dynamic SIF can be deduced from Fig. 7.

The variation of the electric displacement intensity factor with k_0h for various a/h at $h_1 = 10h$ and Dh = 1.0 is depicted in Fig. 8. From this figure, significant overshoot is observed in some specific ranges of

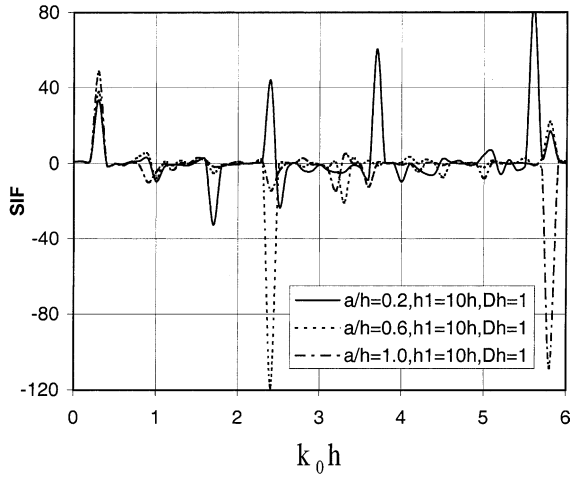

Fig. 4. Normalized SIF versus k_0h for various a/h assuming the permeable boundary condition.

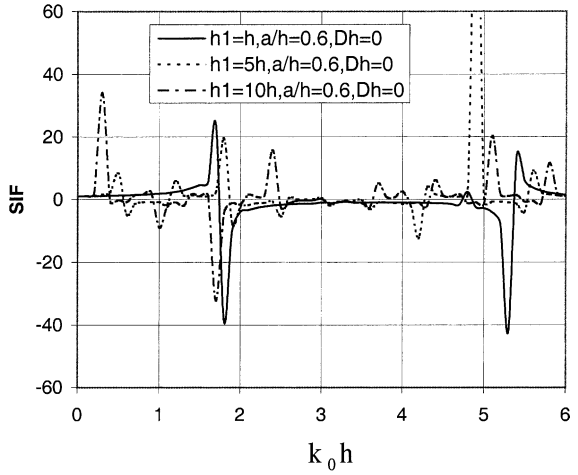

Fig. 5. Normalized SIF versus k_0h for various h_1/h assuming the impermeable boundary condition.

frequencies. This indicates that a strong local electric field is induced at the crack tip, which may further lead to failure of the piezoelectric material.

Fig. 9 compares the solutions for the permeable and impermeable conditions. For lower frequencies, the difference between the two solutions is negligible. However, when the frequency becomes high, the difference is significant.

5.2. The interacting cracks

In this sub-section, we present the results of the two-crack solution. It is assumed that $a_1 = -a$, $b_1 = a$, $a_2 = 2a$ and $b_2 = 4a$. The resulting SIF and EDIF at the inner tip of crack one are shown in Figs. 10–12. The corresponding single crack solution is also depicted in these figures for comparison. It is seen from

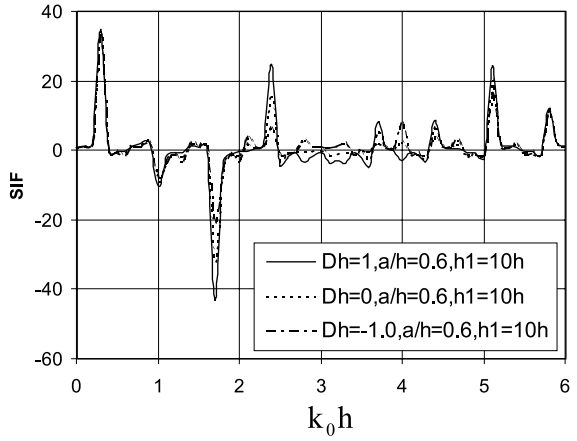

Fig. 6. Normalized SIF versus k_0h for various Dh assuming the impermeable boundary condition.

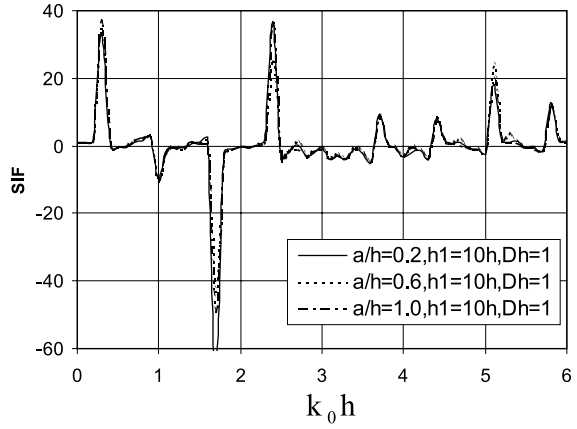

Fig. 7. Normalized SIF versus k_0h for various a/h assuming the impermeable boundary condition.

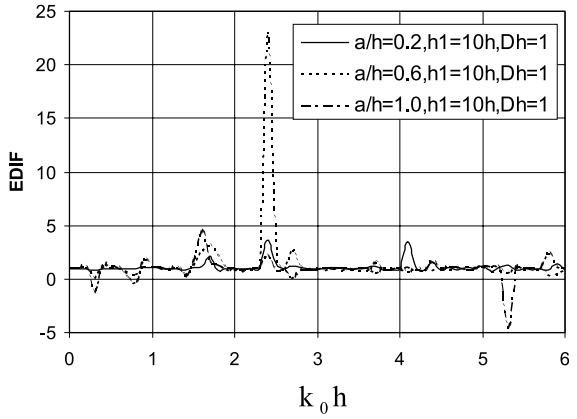

Fig. 8. Normalized EDIF versus k_0h for various a/h assuming the impermeable boundary condition.

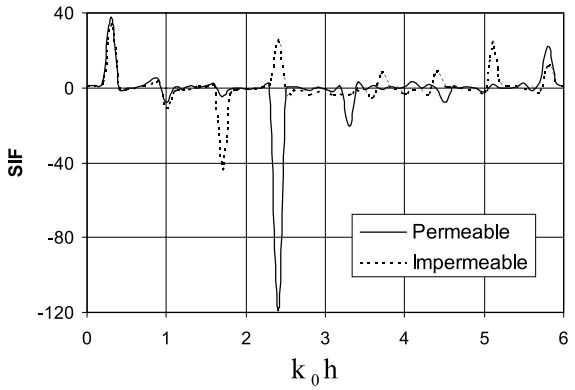

Fig. 9. Comparison between solutions of the permeable and impermeable boundary conditions assuming $a/h = 0.6$, $h_1 = 10h$ and $\mathrm{Dh} = 1$.

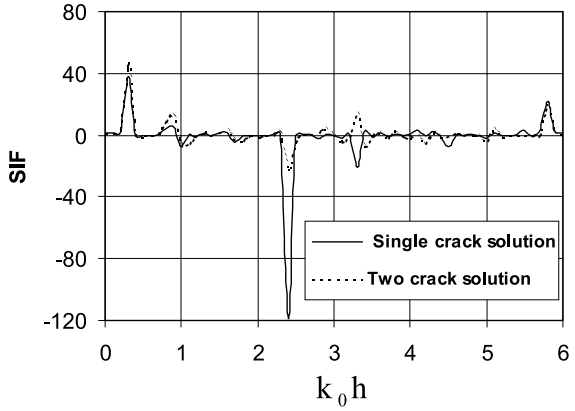

Fig. 10. Normalized SIF versus k_0h assuming the permeable boundary condition with $a/h = 0.6$, $h_1 = 10h$ and $\mathrm{Dh} = 1$.

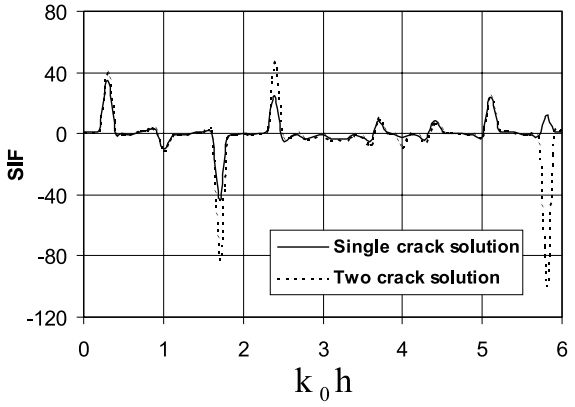

Fig. 11. Normalized SIF versus k_0h assuming the impermeable boundary condition with $a/h = 0.6$, $h_1 = 10h$ and $\mathrm{Dh} = 1$.

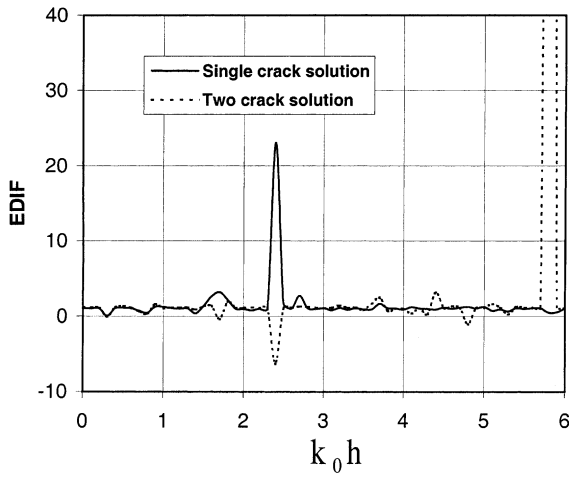

Fig. 12. Normalized EDIF versus k_0h assuming the impermeable boundary condition with $a/h = 0.6$, $h_1 = 10h$ and Dh = 1.

Figs. 10 and 11 that due to the interaction of cracks, the dynamic stress intensity factor may increase or decrease in some ranges of frequencies, depending on the value of k_0h. Similar phenomenon can be observed for the electric displacement intensity factor in Fig. 12.

6. Conclusions

The dynamic behaviour of a piezoelectric laminate containing multiple interfacial cracks subjected to steady-state electro-mechanical loads is investigated. The analysis is based on the use of integral transform techniques and integral equation methods. Numerical calculations are carried out to study the effect of the geometry of the interacting cracks, the applied electric fields, the electric boundary conditions along crack faces and the loading frequency on the resulting dynamic stress intensity factor and electric displacement intensity factor. The study reveals that:

1. Small cracks are more likely to propagate and cause damage to the structure than large cracks when electro-mechanical loads are applied in some specific ranges of frequencies.
2. The presence of either a positive or a negative electric field results in an increase or a decrease of the dynamic stress intensity factor, depending on the frequencies of the applied electro-mechanical loads. This indicates that both a positive electric field and a negative electric field can retard or promote the propagation of a crack.
3. For both the permeable and impermeable boundary conditions, the phenomenon of an intense vibration is observed.
4. When the impermeable boundary condition is considered, a strong local electric field may be induced at the crack tip in some specific ranges of frequencies.
5. For lower frequencies of the applied electro-mechanical loads, both the permeable boundary condition and the impermeable boundary condition give comparable results of local stress fields. When the frequency is high, the difference between the two cases becomes significant and they should be treated separately.
6. Compared with the single crack problem, both the dynamic stress intensity factor and the electric displacement intensity factor may increase or decrease in some ranges of frequencies due to the interaction of cracks.

Acknowledgements

The authors wish to acknowledge Materials and Manufacturing Ontario (MMO), Sensor Technology Limited and Instron Canada for their support of this work.

References

Chen, Z.T., Karihaloo, B.L., 1999. Dynamic response of a cracked piezoelectric ceramic under arbitrary electro-mechanical impact. International Journal of Solids and Structures 36, 5125–5133.

Khutoryyansky, N.M., Sosa, H., 1995. Dynamic representation formulas and fundamental solutions for piezoelectricity. International Journal of Solids and Structures 32, 3307–3325.

Li, S., Mataga, P.A., 1996a. Dynamic crack propagation in piezoelectric materials. Part 1: electrode solution. Journal of the Mechanics and Physics of Solids 44, 1799–1830.

Li, S., Mataga, P.A., 1996b. Dynamic crack propagation in piezoelectric materials. Part 2: vacuum solution. Journal of the Mechanics and Physics of Solids 44, 1831–1866.

Li, X.F., Fan, T.Y., Wu, X.F., 2000. A moving anti-plane crack at the interface between two dissimilar piezoelectric materials. International Journal of Engineering Science 38, 1219–1234.

Meguid, S.A., Chen, Z.T., 2001. Transient response of a finite piezoelectric strip containing coplanar insulating cracks under electro-mechanical impact. Mechanics of Materials 33, 85–96.

Meguid, S.A., Wang, X.D., 1998. Dynamic anti-plane behavior of interacting cracks in a piezoelectric material. International Journal of Fracture 91, 391–403.

Narita, F., Shindo, Y., 1999. Scattering of antiplane shear waves by a finite crack in piezoelectric laminates. Acta Mechanica 134, 27–43.

Norris, A.N., 1994. Dynamic Green's functions in anisotropic piezoelectric, thermoelastic and poroelastic solids. Proceedings of the Royal Society of London A 447, 175–186.

Shin, J.W., Kwon, S.M., Lee, K.Y., 2001. An eccentric crack in a piezoelectric strip under anti-plane shear impact loading. International Journal of Solids and Structures 38, 1483–1494.

Shindo, Y., Ozawa, E., 1990. Dynamic analysis of a cracked piezoelectric material. In: Hsieh, R.K.T. (Ed.), Mechanical Modeling of New Electromagnetic Materials. Elsevier, Amsterdam, pp. 297–304.

Wang, X.D., 2001. On the dynamic behavior of interacting interfacial cracks in piezoelectric media. International Journal of Solids and Structures 38, 815–831.

Wang, X.D., Meguid, S.A., 2000. Modelling and analysis of the dynamic behaviour of piezoelectric materials containing interacting cracks. Mechanics of Materials 32, 723–737.

Wang, X., Yu, S., 2000. Transient response of a crack in a piezoelectric strip subjected to the mechanical and electrical impacts. International Journal of Solids and Structures 37, 5795–5808.

Wang, B.L., Han, J.C., Du, S.Y., 2000. Electroelastic fracture dynamics for multi-layered piezoelectric materials under dynamic anti-plane shearing. International Journal of Solids and Structures 37, 5219–5231.